Received 10 November 2024; revised 11 January 2025; accepted 17 February 2025. Date of publication 4 March 2025;
date of current version 20 March 2025. The review of this article was arranged by Editor K. Cheng.

Digital Object Identifier 10.1109/JEDS.2025.3547860

Channel Length Dependence of Effective Barrier Height Experienced by Charge Carriers in Schottky-Barrier Transistors Based on Si-Nanowire Arrays

DAE-YOUNG JEON[1], SO JEONG PARK[2], SEBASTIAN PREGL[3], JENS TROMMER[3] (Senior Member, IEEE), ANDRÉ HEINZIG[4], THOMAS MIKOLAJICK[3,4] (Fellow, IEEE), AND WALTER M. WEBER[5] (Member, IEEE)

1 Department of Electrical Engineering, Gyeongsang National University, Jinju 52828, Gyeongnam, Republic of Korea
2 Semiconductor Design Examination Division, Korean Intellectual Property Office, Daejeon 35208, Republic of Korea
3 Namlab gGmbH, 01187 Dresden, Germany
4 Chair for Nanoelectronics, Technische Universität Dresden, 01187 Dresden, Germany
5 Institute of Solid State Electronics, TU Wien, 1040 Wien, Austria

CORRESPONDING AUTHOR: D.-Y. JEON (e-mail: dyjeon@gnu.ac.kr)

This work was supported in part by the Research Grant of the Gyeongsang National University in 2024, and in part by the Ministry of Education and National Research Foundation of Korea through the "Convergence and Open Sharing System" Project (the Semiconductor Material, Component, and Equipment).

ABSTRACT Schottky-barrier (SB) transistors show great potential as advanced transistors for meeting power, performance, area, and cost requirements. In this study, the dominant transport mechanisms of SB Si-nanowire (NW) transistors were investigated with respect to channel length for accurate performance estimation and to provide key insights for practical applications. Evaluations of the temperature-dependent drain current, transconductance, and activation energy from SB Si-NW transistors revealed that the SB-dominant thermionic effect competes with Si-NW channel-limited conduction when the initial SB height is relatively low. Moreover, the Si-NW channel length was sufficiently long to dominate the total resistance, overcoming resistance effects arising from the SB.

INDEX TERMS Channel length dependence, channel-limited conduction, Schottky-barrier dominant thermionic effect, Schottky-barrier transistors, Si-nanowires.

I. INTRODUCTION

SCHOTTKY-BARRIER (SB) transistors can mitigate short-channel effects, facilitating improvements in device power, performance, area, and cost because SB contacts enable ultra-shallow junctions and minimize undesirable n-p-n bipolar-transistor action [1], [2], [3], [4]. Additionally, silicided SB junctions produce a steep junction profile with low contact resistance, thereby eliminating the need for high-temperature implantation annealing processes [4], [5], [6]. Ambipolar transport characteristics, involving the injection of both electrons and holes, have been observed primarily in SB transistors with metal silicide contacts. The performance of high-mobility thin-film transistors, pH sensors, biosensors, and steep-slope devices can be enhanced through SB transistors [7], [8], [9], [10]. Furthermore, reconfigurable transistors based on SB junctions enable novel combinational circuit technology, achieving reduced chip area and low thermal budget [11], [12], [13], [14]. Advanced devices incorporating SB contacts and nanomaterials, such as semiconducting nanowires (NWs) and two-dimensional materials, have also been reported [15], [16], [17], [18]. More recently, SB-based field-effect transistors have been integrated into advanced complementary metal-oxide-semiconductor processes, utilizing the superior electrostatics of fully depleted semiconductor-on-insulator technology [19], [20]. Although the physics of SB transistors is generally more complex than that of conventional transistors [3], [21], it is essential to elucidate the dominant transport mechanisms related to scaling properties for accurate performance estimation and the practical application of SB transistors.

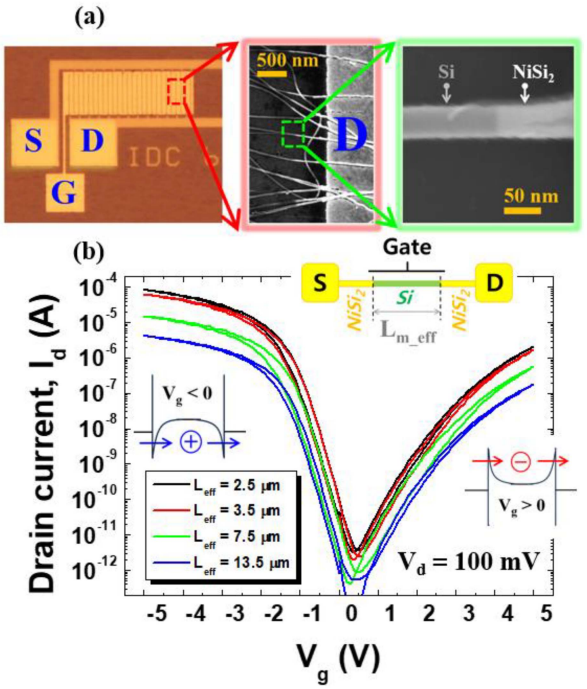

FIGURE 1. **(a) Optical and scanning electron microscopy (SEM) images of the fabricated SB Si-NW transistors, showing a distinct $NiSi_2$/Si-NW heterojunction at the source and drain. (b) Measured transfer curves with varying effective lengths (L_{eff}); the inset illustrates the simplified structure of the SB Si-NW transistors under test. SB: Schottky-barrier; NW: nanowire.**

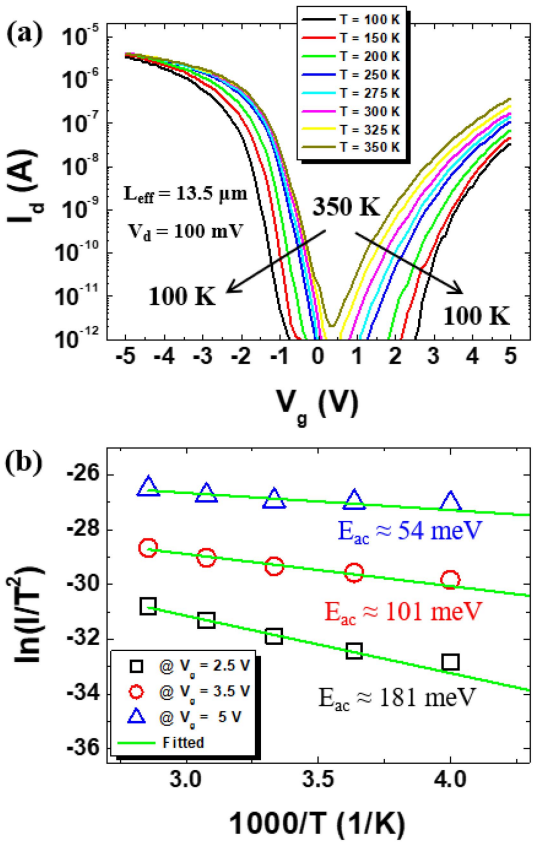

FIGURE 2. **(a) Temperature (T)-dependent transfer curves of the SB Si-NW transistor with an effective device length of L_{eff} = 13.5 μm. (b) Arrhenius plots for various gate voltage (V_g) values in the electron conduction regime, used to extract the activation energy (E_{ac}) based on the following equation: $\ln(I_d/T^2) \approx -q/kT \times E_{ac}(V_g)$.**

In this study, ambipolar SB transistors with bottom-up-grown silicon-nanowire (Si-NW) channels were fabricated to evaluate the effective SB height (φ_{eff}) encountered by charge carriers during transport in relation to the transistor's channel length. The SB-dominant thermionic effects and the Si-NW single-crystal channel-limited conduction regime were clearly influenced by the channel length, as verified by temperature-dependent drain current (I_d), transconductance (g_m), and φ_{eff} estimated from the activation energy (E_{ac}).

II. RESULTS AND DISCUSSION

Figure 1(a) shows optical microscopy and SEM images of the completed ambipolar transistors, constructed from bottom-up-grown Si-NWs with a well-defined $NiSi_2$/Si-NW interface. In the SEM images, the lighter-colored NWs represent $NiSi_2$, whereas darker-colored NWs correspond to the Si channel. The effective device length (L_{eff}), determined using a transfer length method based on the gate-to-channel capacitance (C_{gc}, referencing the linear relationship between C_{gc} and the on-mask channel length), ranged from L_{eff} = 2.5 to 13.5 μm [22]. Details regarding the Si-NW growth method and device fabrication process, including silicidation, are provided in previous studies [18], [22].

Transfer curves of I_d versus gate voltage (V_g) for the fabricated SB Si-NW transistors were measured at different L_{eff} values, as shown in Fig. 1(b), in the linear operation regime with a small drain bias (V_d = 100 mV). The schematic in Fig. 1(b) illustrates a simplified diagram of the SB Si-NW transistors with source (S), drain (D), and gate (G) connections for measurements. The transfer curves in Fig. 1(b) display the asymmetric ambipolar characteristics of carrier transport because the SB formed by the $NiSi_2$/Si heterojunction enables both electron and hole injection, as shown in the energy band diagram of the inset in Fig. 1(b). The Fermi level of $NiSi_2$ lies farther from the conduction band than from the valence band of the Si-NW [5], [6]. In fact, the temperature dependence of I_d-V_g for hole conduction was very different from that for electron conduction. The effective barrier height for holes was much smaller compared to electrons at the same $|V_g|$. This will be discussed in more detail in Fig. 2 and Fig. 3.

Figure 2(a) shows the temperature-dependent transfer curves of an SB Si-NW transistor with a long channel (L_{eff} = 13.5 μm). The electrical measurements as a function of temperature were performed using a cryogenic probe station from Lake Shore Cryotronics, which is a continuous refrigeration system using liquid nitrogen to provide efficient low-temperature operational control. I_d increased with temperature from T = 100 K to 350 K due to enhanced thermionic emission of charge carriers through the SB interface. The rate of increase in I_d was much larger in

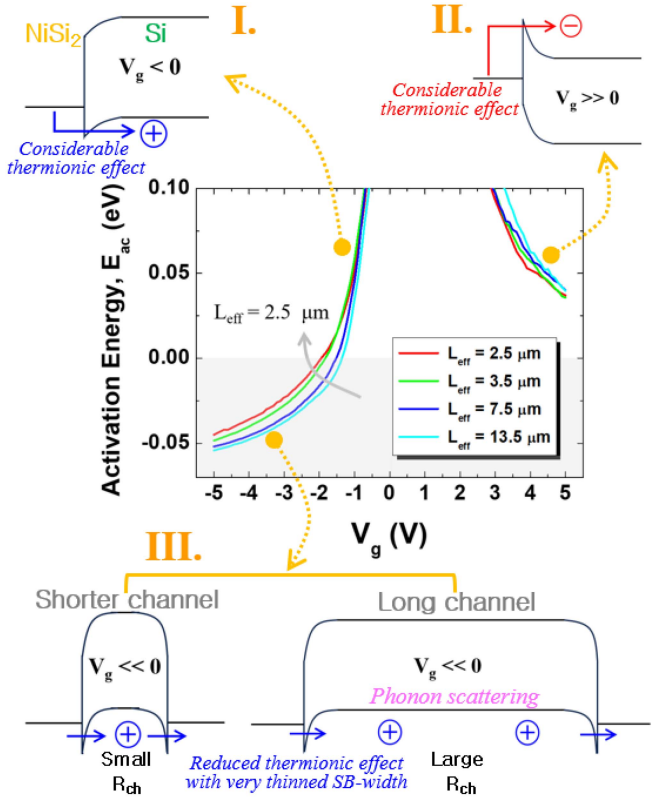

FIGURE 3. Extracted activation energy (E_{ac}) of SB Si-NW transistors with varying L_{eff}. The schematic diagram of the energy band illustrates the dominant conduction mechanism in each operating regime.

the electron conduction regime ($V_g > 0$) than in the hole conduction regime ($V_g < 0$), considering that the SB height ($q\varphi_{Be} \approx 0.66$ eV) for electrons was higher than that for holes ($q\varphi_{Bh} \approx 0.46$ eV) at the $NiSi_2$/Si junction [5], [6]. With respect to $V_g < 0$, the injection probability of hole charge carriers increased due to the combined effects of thermionic emission and temperature-independent tunneling through the SB. Conversely, electron injection, primarily dependent on thermionic emission, was enhanced for $V_g > 0$. Given the substantial initial SB height, the thermionic emission mechanism dominated carrier transport relative to tunneling.

Arrhenius plots for various V_g values in the electron conduction regime ($V_g > 0$) are shown in Fig. 2(b). E_{ac} was extracted using a linear dependency of $\ln(I/T^2)$ versus 1000/T, based on the equation $\ln(I_d/T^2) \approx -q/kT \times E_{ac}(V_g)$, where k is Boltzmann's constant. E_{ac} was strongly correlated with φ_{eff}. A relatively small E_{ac} value of 54 meV was obtained at $V_g = 5$ V. As V_g increased, the effective width of the SB decreased, increasing the tunneling current through the thinned SB and thus reducing φ_{eff}.

The E_{ac} for electron and hole conduction characteristics of SB Si-NW transistors with varying L_{eff} were extracted across the entire operating regime, as shown in Fig. 3. As expected, all extracted E_{ac} values in the electron conduction regime ($V_g > 0$) were positive, representing a considerable thermionic effect. Additionally, E_{ac} decreased as V_g increased due to the enhanced tunneling current through the thinned SB at a higher V_g. This result demonstrates the typical behavior of SB transistors, governed by the charge carrier transmissibility through the SB (note II. schematic diagram of energy band) [4], [21], [23], [24], [25]. Notably, no significant difference was observed in the temperature dependence trend for electron transport across different L_{eff} values, indicating primarily SB-limited conduction.

In contrast, a substantially different trend was observed in the hole conduction regime ($V_g < 0$). With decreasing V_g, the extracted E_{ac} decreased in a similar manner due to the increased injection of holes through the thinned SB (note I. schematic diagram of energy band). However, at $V_g < -1.5$ V, a negative E_{ac} value was obtained, as shown in the gray-colored region of the plot in Fig. 3. The negative E_{ac} value suggests that the SB-limited thermionic effect is no longer the dominant conduction mechanism. When the resistance originating from the SB becomes lower than that of the channel, Si-channel-dominated conduction can limit the current, even in SB Si-NW transistors, as is well known from conventional inversion channel transistors with ohmic-like contacts [26], [27]. As the effective SB width for hole transport approaches a minimum value at $V_g < -1.5$ V, the contact resistance due to the SB becomes smaller than the resistance of the single-crystalline Si-NW channel. Consequently, phonon-scattering-dominant conduction becomes more pronounced and competes with the thermionic effect from the SB (note III. schematic diagram of energy band). Charge transport in single-crystal semiconductors is dominated by phonon scattering; as temperature decreases, fewer holes are scattered by phonons, resulting in an increase in I_d flow [4]. Due to the relatively low initial SB height ($q\varphi_{Bh} \approx 0.46$ eV), V_g more readily produced a minimum SB width for hole conduction; thus, negative E_{ac} values were only extracted from the hole conduction regime. In Figure 2, the hole current near $V_g = -5$ V showed little change, but the electron current near $V_g = 5$ V decreased significantly with decreasing temperature, which is attributed to the fact that the thermionic hole current decreases and at the same time the phonon scattering decreases, which can enhance the hole current at lower temperatures. Indeed, it was also found that the hole current increases with decreasing temperature, with a zero-temperature coefficient point under high drain bias [27]. Intriguingly, a longer channel length resulted in larger negative E_{ac} values for the same V_g because the longer channel is more susceptible to the resistive effects of the Si-NW channel. Urban et al. also reported an I_d dependence on gate length for SB transistors, as demonstrated in silicon-on-insulator devices with relatively small SB values [28].

Figure 4 shows the temperature-dependent g_m of SB Si-NW transistors with varying L_{eff}. In the electron conduction regime ($V_g > 0$), g_m increased with temperature regardless of channel length, as shown in Fig. 4(b) and 4(d). SB-dominated conduction for electrons gave rise to no significant changes on temperature dependence of g_m as

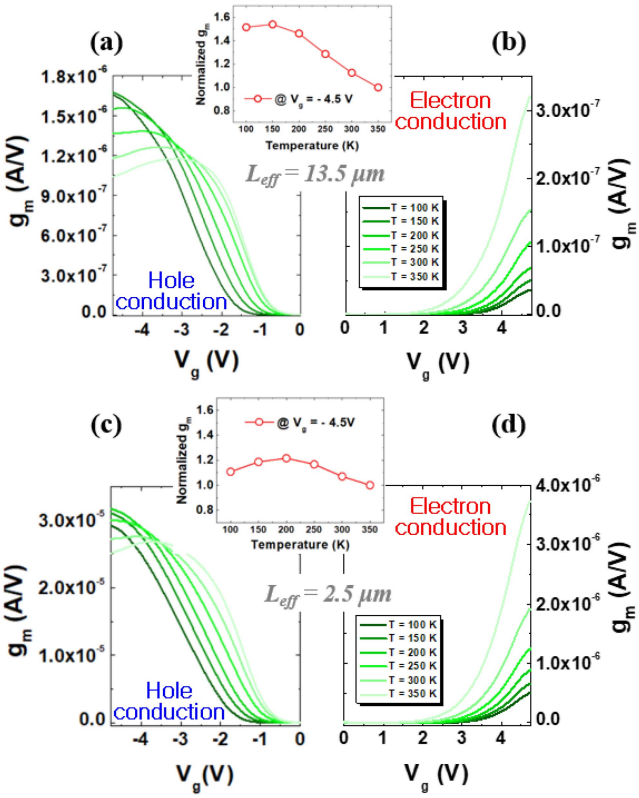

FIGURE 4. **Temperature-dependent transconductance (g_m) of SB Si-NW transistors with varying L_{eff}. (a) Hole conduction regime and (b) electron conduction regime in a device with a long channel (L_{eff} = 13.5 μm). (c) Hole conduction regime and (d) electron conduction regime with a shorter channel (L_{eff} = 2.5 μm).**

varying device lengths. In the hole conduction regime with $V_g < -4$ V, where an ohmic-like contact could be formed with a clearly negative value of E_{ac} in Fig. 3, g_m decreased as temperature increased, shown in Fig. 4(a). In conventional Si inversion-mode transistors, the effective mobility trend is similar to that for g_m [29]. In these transistors, effective mobility decreases with increasing temperature due to the dominance of phonon scattering in the single-crystalline Si channel at higher temperatures [4], [30]. The inset of Fig. 4(a) illustrates typical phonon-scattering-dominant behavior and Si-NW channel-limited conduction in SB Si-NW transistors under bias conditions for hole carriers. Only a slight change in g_m was observed in SB Si-NW transistors with a shorter channel length, as shown in the inset of Fig. 4(c). In these shorter devices, the SB thermionic effect and phonon scattering from the Si-NW channel likely have comparable influences. The length dependence on the temperature trend of g_m indicates clearly Si-channel-confined conduction for hole transport, not SB-confined conduction.

III. CONCLUSION

SB transistors based on a parallel array of bottom-up grown Si-NWs were fabricated, and their operating mechanisms were evaluated with respect to channel length using temperature-dependent I–V characteristics over the range of 100 to 350 K. In the electron conduction regime, the extracted E_{ac} exhibited a positive value, indicating a significant thermionic effect from the SB, as expected. Additionally, the E_{ac} trend for electron transport remained consistent across different channel lengths. In contrast, a negative E_{ac} value was observed in the hole conduction regime; longer channel lengths led to a larger negative E_{ac} value at the same V_g. Notably, V_g more readily induced a minimum SB width for hole conduction due to the initially lower SB height (i.e., 0.46 eV for holes and 0.66 eV for electrons). When the resistance effect due to the SB became smaller than that of the single-crystalline Si-NW channel, Si-channel-dominated hole conduction occurred even in SB-based Si-NW transistors. Moreover, the temperature-dependent g_m of SB Si-NW transistors with a long channel length exhibited Si-NW channel-limited conduction, with typical phonon scattering behavior in hole transport.

REFERENCES

[1] M. Badaroglu et al., *IEEE International Roadmap for Devices and Systems 2023 Update*. 2023. [Online]. Available: https://irds.ieee.org/editions/2023
[2] J. M. Shannon and E. G. Gerstner, "Source-gated thin-film transistors," *IEEE Electron Device Lett.*, vol. 24, no. 6, pp. 405–407, Jun. 2003, doi: 10.1109/LED.2003.813379.
[3] M. Schwarz et al., "The Schottky barrier transistor in emerging electronic devices," *Nanotechnology*, vol. 34, no. 35, 2023, Art. no. 352002, doi: 10.1088/1361-6528/acd05f.
[4] S. M. Sze, Y. Li, and K. K. Ng, *Physics of Semiconductor Devices*. Hoboken, NJ, USA: Wiley, 2021, doi: 10.1002/0470068329.
[5] A. Heinzig, S. Slesazeck, F. Kreupl, T. Mikolajick, and W. M. Weber, "Reconfigurable silicon nanowire transistors," *Nano Lett.*, vol. 12, no. 1, pp. 119–124, 2012, doi: 10.1021/nl203094h.
[6] T. Mikolajick et al., "Silicon nanowires–A versatile technology platform," *Physica Status Solidi (RRL)–Rapid Res. Lett.*, vol. 7, no. 10, pp. 793–799, 2013, doi: 10.1002/pssr.201307247.
[7] F. M. Zörgiebel et al., "Schottky barrier-based silicon nanowire pH sensor with live sensitivity control," *Nano Res.*, vol. 7, pp. 263–271, Jan. 2014, doi: 10.1007/s12274-013-0393-8.
[8] D. Karnaushenko et al., "Light weight and flexible high-performance diagnostic platform," *Adv. Healthcare Mater.*, vol. 4, no. 10, pp. 1517–1525, 2015, doi: 10.1002/adhm.201500128.
[9] J. Schutt et al., "Compact nanowire sensors probe microdroplets," *Nano Lett.*, vol. 16, no. 8, pp. 4991–5000, 2016, doi: 10.1021/acs.nanolett.6b01707.
[10] J. Zhang, J. Trommer, W. M. Weber, P.-E. Gaillardon, and G. De Micheli, "On temperature dependency of steep subthreshold slope in dual-independent-gate FinFET," *IEEE J. Electron Devices Soc.*, vol. 3, pp. 452–456, 2015, doi: 10.1109/JEDS.2015.2482123.
[11] A. Heinzig, T. Mikolajick, J. Trommer, D. Grimm, and W. M. Weber, "Dually active silicon nanowire transistors and circuits with equal electron and hole transport," *Nano Lett.*, vol. 13, no. 9, pp. 4176–4181, 2013, doi: 10.1021/nl401826u.
[12] G. Galderisi, T. Mikolajick, and J. Trommer, "The RGATE: An 8-in-1 polymorphic logic gate built from reconfigurable field effect transistors," *IEEE Electron Device Lett.*, vol. 45, no. 3, pp. 496-499, Mar. 2024, doi: 10.1109/LED.2023.3347397.
[13] T. Mikolajick et al., "Reconfigurable field effect transistors: A technology enablers perspective," *Solid-State Electron.*, vol. 194, Aug. 2022, Art. no. 108381, doi: 10.1016/j.sse.2022.108381.
[14] L. Wind et al., "Reconfigurable Si field-effect transistors with symmetric on-states enabling adaptive complementary and combinational logic," *IEEE Trans. Electron Devices*, vol. 71, no. 2, pp. 1302–1307, Feb. 2024.
[15] H. Tian et al., "Novel field-effect Schottky barrier transistors based on graphene-MoS_2 heterojunctions," *Sci. Rep.*, vol. 4, no. 1, p. 5951, 2014, doi: 10.1038/srep05951.

[16] S. Das, H.-Y. Chen, A. V. Penumatcha, and J. Appenzeller, "High performance multilayer MoS_2 transistors with scandium contacts," *Nano Lett.*, vol. 13, no. 1, pp. 100–105, 2013, doi: 10.1021/nl303583v.

[17] Z. Wang et al., "The ambipolar transport behavior of WSe_2 transistors and its analogue circuits," *NPG Asia Mater.*, vol. 10, no. 8, pp. 703–712, 2018, doi: 10.1038/s41427-018-0062-1.

[18] S. Pregl et al., "Parallel arrays of Schottky barrier nanowire field effect transistors: Nanoscopic effects for macroscopic current output," *Nano Res.*, vol. 6, pp. 381–388, May 2013, doi: 10.1007/s12274-013-0315-9.

[19] V. Sessi et al., "S2–2 back-bias reconfigurable field effect transistor: A flexible add-on functionality for 22 nm FDSOI," in *Proc. Silicon Nanoelectron. Workshop (SNW)*, 2021, pp. 1–2.

[20] M. Simon et al., "Three-to-one analog signal modulation with a single back-bias-controlled reconfigurable transistor," *Nat. Commun.*, vol. 13, no. 1, p. 7042, 2022, doi: 10.1038/s41467-022-34533-w.

[21] L. E. Calvet, "Electrical transport in Schottky barrier MOSFETs," Ph.D. dissertation, Dept. Electr. Eng., Yale Univ., New Haven, CT, USA, 2001.

[22] D.-Y. Jeon et al., "Scaling and graphical transport-map analysis of ambipolar Schottky-barrier thin-film transistors based on a parallel array of Si nanowires," *Nano Lett.*, vol. 15, no. 7, pp. 4578–4584, 2015, doi: 10.1021/acs.nanolett.5b01188.

[23] J. Beister, A. Wachowiak, A. Heinzig, J. Trommer, T. Mikolajick, and W. M. Weber, "Temperature dependent switching behaviour of nickel silicided undoped silicon nanowire devices," *Physica Status Solidi (C)*, vol. 11, nos. 11–12, pp. 1611–1617, 2014, doi: 10.1002/pssc.201400055.

[24] G. Galderisi, C. Beyer, T. Mikolajick, and J. Trommer, "Insights into the temperature-dependent switching behavior of three-gated reconfigurable field-effect transistors," *Physica Status Solidi (A)*, vol. 220, no. 13, 2023, Art. no. 2300019, doi: 10.1002/pssa.202300019.

[25] R. Behrle et al., "Understanding the electronic transport of Al–Si and Al–Ge nanojunctions by exploiting temperature-dependent bias spectroscopy," *ACS Appl. Mater. Interfaces*, vol. 16, no. 15, pp. 19350–19358, 2024, doi: 10.1021/acsami.3c18674.

[26] D. Qiu and E. K. Kim, "Electrically tunable and negative Schottky barriers in multi-layered graphene/MoS_2 heterostructured transistors," *Sci. Rep.*, vol. 5, no. 1, 2015, Art. no. 13743, doi: 10.1038/srep13743.

[27] D.-Y. Jeon et al., "In-depth electrical characterization of carrier transport in ambipolar Si-NW Schottky-barrier FETs," in *Proc. 47th Eur. Solid-State Device Res. Conf. (ESSDERC)*, 2017, pp. 304–307, doi: 10.1109/ESSDERC.2017.8066652.

[28] C. Urban, C. Sandow, Q.-T. Zhao, J. Knoch, S. Lenk, and S. Mantl, "Systematic study of Schottky barrier MOSFETs with dopant segregation on thin-body SOI," *Solid-State Electron.*, vol. 54, no. 2, pp. 185–190, 2010, doi: 10.1016/j.sse.2009.12.017.

[29] F. Balestra and G. Ghibaudo, "Brief review of the MOS device physics for low temperature electronics," *Solid-State Electron.*, vol. 37, no. 12, pp. 1967–1975, 1994, doi: 10.1016/0038-1101(94)90064-7.

[30] G. Ghibaudo, "Critical MOSFETs operation for low voltage/low power IC's: Ideal characteristics, parameter extraction, electrical noise and RTS fluctuations," *Microelectron. Eng.*, vol. 39, nos. 1–4, pp. 31–57, 1997, doi: 10.1016/S0167-9317(97)00166-4.